

Inhibitory effect of DNA structure on the efficiency of reaction of guanosine moieties with a nitrenium ion

Michael Novak* and Sonya A. Kennedy

Department of Chemistry, Miami University, Oxford, Ohio 45056, USA

Received 30 April 1997; revised 8 July 1997; accepted 11 July 1997

ABSTRACT: The *N*-acetyl-*N*-(2-fluorenyl)nitrenium ion (**2a**) reacts very efficiently with monomeric 2'-deoxyguanosine (d-G) to form a C-8 adduct, *N*-(2'-deoxyguanosin-8-yl)-2-acetylaminofluorene (**6**), in an aqueous environment, with a selectivity ratio, k_{d-G}/k_s , of $13.1 \times 10^3 \text{ M}^{-1}$ at 0°C and $4.8 \times 10^3 \text{ M}^{-1}$ at 30°C. The reactivity of the self-complementary oligomer d-ATGCAT with **2a** can be separated into components due to the single-stranded (SS) and double-stranded (DS) forms. Within the error limits of the measurements $k_{SS}/k_{d-G} \approx 0.27$ and $k_{DS}/k_{d-G} \approx 0$. Another measure of the reactivity of d-G moieties in the DNA double helix can be obtained from measurements with the circular super-coiled plasmid pUC19. This plasmid provides an upper limit for k_{pUC19}/k_{d-G} of 0.02, where k_{pUC19} is the average trapping rate constant per d-G moiety in pUC19. The strong inhibition of the trapping reaction caused by the tertiary structure of the DNA double helix may be responsible for the change in product distribution of **2a**-d-G adducts found from reaction with d-G, and denatured DNA (exclusive C-8 adduct, **6**) and native DNA [5–20% N-2 adduct, 3-(2'-deoxyguanosin-*N*²-yl)-2-acetylaminofluorene, **7**]. © 1998 John Wiley & Sons, Ltd.

KEYWORDS: guanosine; nitrenium; DNA structure

INTRODUCTION

The 'azide clock' method has been used to characterize the lifetimes and relative reactivities of carbocations in nucleophilic solvents for over 25 years,¹ and was first used to characterize the lifetime of a nitrenium ion about 10 years ago.² Using this method, we have recently shown that certain carcinogenic esters of *N*-arylhydroxylamines and *N*-arylhydroxamic acids (**1**) decompose in aqueous solution into nitrenium ions (**2**) that react very selectively with N_3^- .^{3,4} These ions also react efficiently with 2'-deoxyguanosine (d-G).⁵ Direct measurements of the aqueous solution lifetimes of **2a–c** confirm that the ions have lifetimes in the range 0.1–10 μs, and that they react with N_3^- with rate constants of *ca* $5 \times 10^9 \text{ M}^{-1} \text{ s}^{-1}$.^{6,7}

Although it is known that **2a–c** react efficiently with d-G, and the C-8 adducts generated from reaction with monomeric d-G are equivalent to the major adducts isolated from *in vivo* and *in vitro* experiments with DNA,^{5,8,9} the effect of DNA structure on the adduct-forming reaction is unknown. In particular, it is not known if the tertiary structure of the DNA double helix

promotes or inhibits the formation of the d-G–nitrenium ion adducts.

We have compared the selectivity of reactions of the *N*-acetyl-*N*-(2-fluorenyl)nitrenium ion, (**2a**) with monomeric d-G, the self-complementary hexamer d-ATGCAT and the circular super-coiled plasmid pUC19. Our results show that single-stranded DNA retains significant reactivity toward **2a** (*ca* 27% of that of d-G), but that double-stranded DNA has negligible reactivity toward this nitrenium ion. The implications of these results with respect to carcinogenesis are discussed.



a Ar = 2-fluorenyl Y = Ac X = SO_3^-

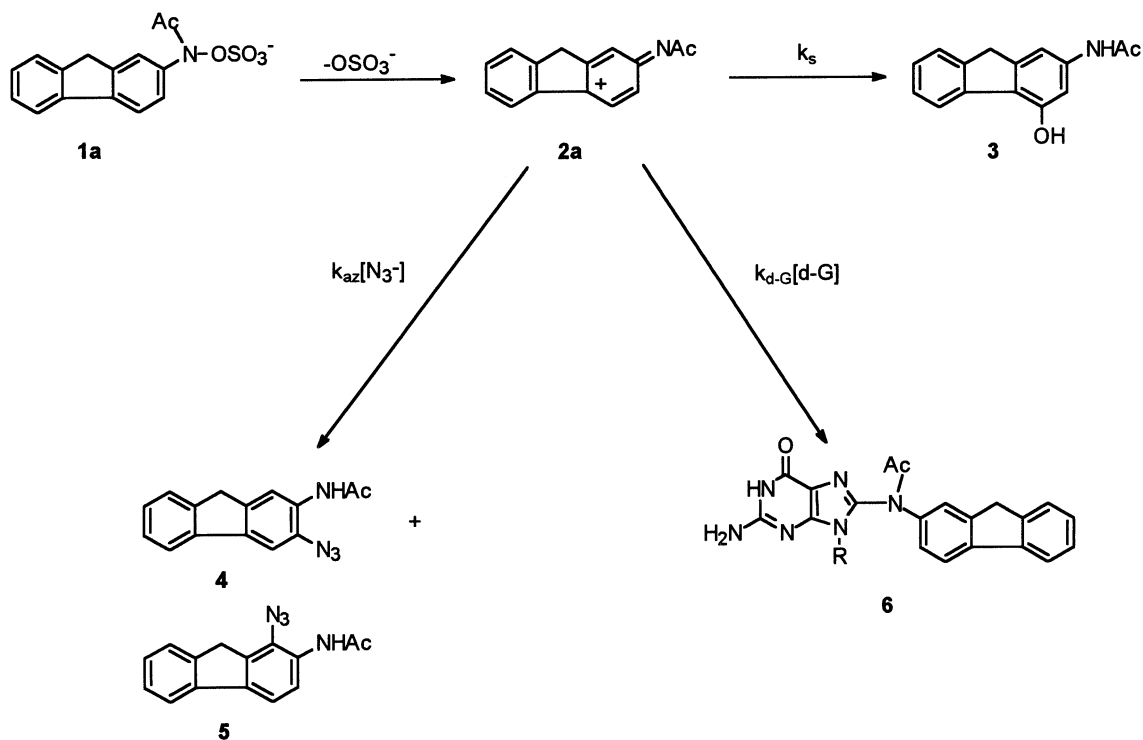
b Ar = 4-biphenyl Y = Ac X = SO_3^-

c Ar = 4-biphenyl Y = H X = C(O)C(CH₃)₃

*Correspondence to: M. Novak, Department of Chemistry, Miami University, Oxford, Ohio 45056, USA.

Email: minovak@miamiu.muohio.edu

Contract/grant sponsor: American Cancer Society; contract grant number: CN-23K.



Scheme 1

RESULTS AND DISCUSSION

The carcinogenic ester **1a** decomposes via rate-limiting heterolytic N—O bond cleavage into the nitrenium ion **2a**, that is efficiently trapped by N_3^- and d-G (Scheme 1).^{3–5} The rate constant ratios k_{az}/k_s and $k_{\text{d-G}}/k_s$ can be determined by measurement of the product yields of the major hydrolysis product **3** and the azide adducts **4** and **5**, or the d-G adduct, **6**, as a function of $[\text{N}_3^-]$ or [d-G].^{3,4,5} In particular, the fractional yield of hydrolysis products, f_s , is given by

$$f_s = \frac{k_s}{k_s + k_x[\text{X}]} \quad (1)$$

where X can be N_3^- , d-G or any other nucleophile that reacts irreversibly with **2a**. The inverse of equation (1):

$$\frac{1}{f_s} = 1 + \frac{k_x}{k_s}[\text{X}] \quad (2)$$

provides a convenient means to evaluate k_x/k_s by linear regression methods.

Figure 1 shows $1/f_s$ as a function of $[\text{N}_3^-]$ for the hydrolysis of **1a** in 1 mM Na_2HPO_4 – NaH_2PO_4 buffer [pH 7.5, $\mu = 0.5$ (NaClO_4)] at 0 and 30°C. Values of k_x/k_s measured at three temperatures for X = N_3^- and d-G are given in Table 1 and $\ln(k_x/k_s)$ is plotted vs $1/T$ in Figure 2. The slopes of the linear correlation lines in Figure 2 are $(\Delta H_s^\ddagger - \Delta H_x^\ddagger)/R$. The lines are parallel within experimental error with $\Delta H_s^\ddagger - \Delta H_{\text{az}}^\ddagger = 5.4 \pm 1.0 \text{ kcal mol}^{-1}$ and $\Delta H_s^\ddagger - \Delta H_{\text{d-G}}^\ddagger = 5.2 \pm 1.2 \text{ kcal mol}^{-1}$ (1 kcal =

4.184 kJ). Since $\Delta H_{\text{az}}^\ddagger \approx \Delta H_{\text{d-G}}^\ddagger$, the most significant difference in these two trapping reactions is due to ΔS^\ddagger . From the intercepts of the plots, $\Delta S_{\text{d-G}}^\ddagger - \Delta S_{\text{az}}^\ddagger = -3.8 \text{ eu}$.

The trapping of **2a** by N_3^- occurs at, or very near, the diffusion limit. Directly measured k_{az} for **2a** generated by laser flash photolysis at 20°C under these conditions is $4.2 \times 10^9 \text{ M}^{-1} \text{ s}^{-1}$.⁶ The measured values of k_{az} at 20°C for several nitrenium ions, including **2a**, with lifetimes ($1/k_s$) of 0.2–30 μs are in the range 4.0×10^9 – $5.0 \times 10^9 \text{ M}^{-1} \text{ s}^{-1}$.^{6,7} This is very similar to diffusion-limited second-order rate constants for trapping of carbocations by N_3^- and other small, strong nucleophiles.¹⁰

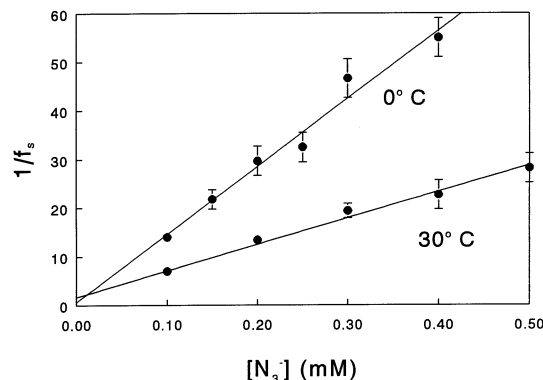


Figure 1. Plot of $1/f_s$ vs $[\text{N}_3^-]$ for **1a** at 0 and 30°C. Regression lines were determined from a weighted least-squares fit

Table 1. Measured values of k_x/k_s at different temperatures

Temperature (°C)	k_x/k_s (M^{-1}) ^a		
	X = N ₃ ^{-b}	X = d-G	X = d-ATGCAT
0	$(14.0 \pm 1.0) \times 10^4$	$(13.1 \pm 1.0) \times 10^3$	$(7.5 \pm 0.4) \times 10^2$
20	$(6.2 \pm 0.4) \times 10^4$ ^c	$(8.0 \pm 0.6) \times 10^3$ ^d	
30	$(5.4 \pm 0.4) \times 10^4$	$(4.8 \pm 0.4) \times 10^3$	$(12.5 \pm 1.0) \times 10^2$

^a Conditions: 1 mM Na₂HPO₄-NaH₂PO₄ aqueous buffer, pH 7.5, $\mu = 0.5$ (NaClO₄), unless indicated otherwise.

^b Solvent was 5 vol.% CH₃CN-H₂O.

^c Ref. 1

^d Ref. 3.

Competition experiments show that the diffusion-limited rate constant for reaction of purine nucleosides with the nitrenium ions **2b** and **2c** at 20°C under these conditions is *ca* $2.0 \times 10^9 M^{-1} s^{-1}$.⁸ Since k_s for **2a** has been measured as $7.7 \times 10^4 s^{-1}$ under these conditions,⁶ k_{d-G} for **2a** at 20°C is *ca* $6.2 \times 10^8 M^{-1} s^{-1}$. This is within a factor of three of the apparent diffusion limit. Since both k_{az} and k_{d-G} are so close to their respective diffusion-controlled limits, it is not surprising that the major differences in these rate constants appear in ΔS^\ddagger .

The rate constant ratios for trapping of **2a** by the oligomer d-ATGCAT were determined by monitoring the change in concentration of the hydrolysis product **3** as a function of [d-ATGCAT]. Figure 3 shows a plot of $1/f_s$ as a function of [d-ATGCAT] at 0 and 30°C. The derived values of $k_{d-ATGCAT}/k_s$ are given in Table 1 and $\ln(k_{d-ATGCAT}/k_s)$ is plotted in Figure 2. The trapping product was not characterized in this case, but it has been shown previously that short DNA oligomers react with **1a** and other esters of *N*-arylhydroxamic acids and *N*-arylhydroxylamines to generate the C-8 guanosine adduct analogous to **6** as the major observed product.⁹

In the absence of oligomer the hydrolysis rate constant, k_0 , for **1a** is $0.010 \pm 0.002 s^{-1}$ at 0°C. In the presence of 0.9 mM d-ATGCAT the rate constant is unchanged at $0.010 \pm 0.001 s^{-1}$. Under these conditions the yield of the hydrolysis product, **3**, is reduced by 40% from its

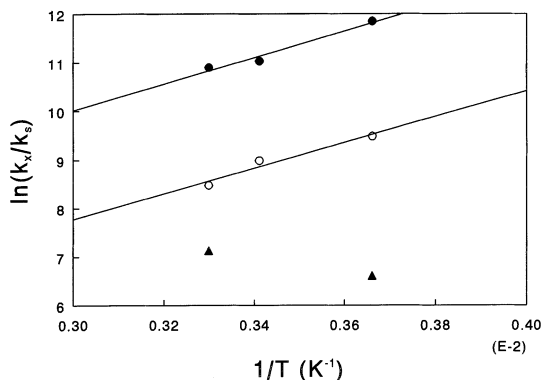


Figure 2. Plot of $\ln(k_x/k_s)$ vs $1/T$. X = (●) N₃⁻, (○) d-G and (▲) d-ATGCAT. Regression lines were determined from an unweighted least-squares fit

yield in the absence of the oligomer. These results are similar to those reported previously for the hydrolysis of **1a** and similar esters in the presence of N₃⁻ and d-G,³⁻⁵ and are consistent with trapping of the nitrenium ion **2a** after rate-limiting N—O bond heterolysis.

The temperature dependence of $k_{d-ATGCAT}/k_s$ is different from that observed for N₃⁻ and d-G. For both of these nucleophiles k_x/k_s decreases with increasing temperature, but the opposite is true for $k_{d-ATGCAT}/k_s$ (Figure 2). A melting curve for d-ATGCAT (Figure 4) shows that in this temperature range the self-complementary oligomer changes from predominantly double-stranded at 0°C (72% double-stranded) to predominantly single-stranded at 30°C (5% double-stranded). These estimates were made in the standard fashion as indicated in Figure 4. We conclude that the temperature dependence of $k_{d-ATGCAT}/k_s$ is caused by the melting of the oligomer dimer over this temperature range, and that the single-stranded form of the oligomer is much more reactive toward the nitrenium ion than is the double-stranded form.

A quantitative estimate of the relative reactivities of the double- and single-stranded forms of the oligomer toward **2a** can be obtained as follows. If x and y are the relative reactivities of the d-G residues in the double- and single-stranded forms, respectively, compared with monomeric d-G, we can write the equation

$$(DS)x + (SS)y = \frac{k_{d-ATGCAT}/k_s}{k_{d-G}/k_s} \quad (3)$$

where DS and SS are the fraction of the oligomer in the double- and single-stranded forms, respectively, at a given temperature as determined from the melting curve. The rate constant ratios $k_{d-ATGCAT}/k_s$ and k_{d-G}/k_s are measured at the same temperature as DS and SS. If we assume that x and y are temperature independent over the narrow temperature range employed here, we can solve simultaneous equations to obtain x and y . The assumption that x and y are temperature independent is equivalent to assuming that the rate constants for trapping of **2a** by the double- and single-stranded forms, k_{DS} and k_{SS} , vary with temperature in the same way that k_{d-G} does. This is probably not true over a large temperature range, but if

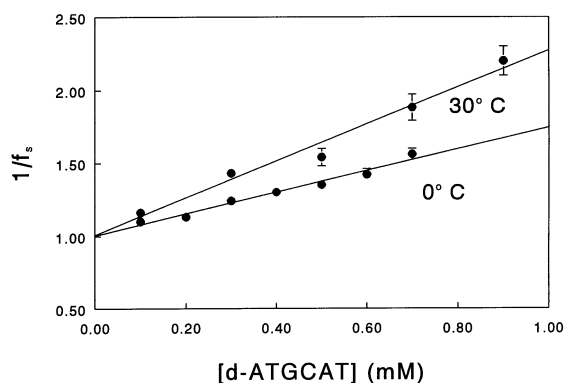


Figure 3. Plot of $1/f_s$ vs $[d\text{-ATGCAT}]$ for **1a** at 0 and 30°C. Regression lines were determined from a weighted least-squares fit

the data are taken over a fairly narrow temperature range this assumption will not lead to major errors. The values of x and y calculated from our data are $-0.02 \approx 0$ and 0.27, respectively. Within the error limits of our experiment we conclude that $k_{DS} \approx 0$ and $k_{SS} = 0.27 k_{d-G}$.

The double-stranded oligomer has very little reactivity toward the nitrenium ion, but the actual level of reactivity is difficult to determine with precision because of the presence of the much more reactive single-stranded form. The selectivity of the double-stranded super-coiled plasmid pUC19 provides another estimate of the reactivity of d-G residues within double-stranded DNA. At 0°C in the presence of sufficient pUC19 to produce a solution 0.66 mM in d-G residues, the yield of the hydrolysis product **3** is reduced by $14.7 \pm 0.5\%$, while k_0 remains constant at *ca* 0.010 s^{-1} . This result corresponds to a value of k_{pUC19}/k_s of $260 \pm 10 \text{ M}^{-1}$, where k_{pUC19} is the trapping rate constant per d-G moiety in pUC19. This is an upper limit since **2a** can react with the small amount of nicked DNA present in the sample and can also bind non-specifically to the phosphate backbone of the DNA.¹¹ Since the reactivity of nitrenium ions with the monomeric purine and pyrimidine bases d-A, d-C and d-T is negligible, these probably do not contribute

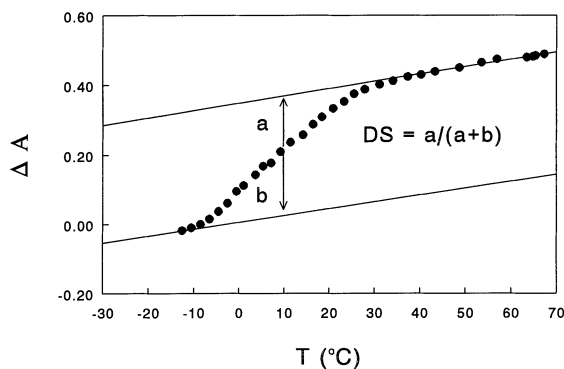


Figure 4. Melting curve for d-ATGCAT at pH 7.5 (5 mM $\text{Na}_2\text{HPO}_4\text{-NaH}_2\text{PO}_4$ buffer), $\mu = 0.5$ (NaClO_4). Absorbance measurements were made at 260 nm

TABLE 2. Relative reactivities of pUC19, d-ATGCAT and d-G toward the nitrenium ion **2a** at 0°C

	k_x/k_{d-G}	Trapping at 0.10 mM in d-G residues (%) ^a
d-G	1	57 ± 3
d-ATGCAT ^b	0.27	26 ± 3
(d-ATGCAT) ₂ ^c	~ 0	~ 0
pUC19	<0.02	$<2.6 \pm 0.2$

$$^a \text{ Calculated from \% trapping} = \frac{k_x/k_s[X](100\%)}{1 + k_x/k_s[X]}$$

^b The single-stranded form.

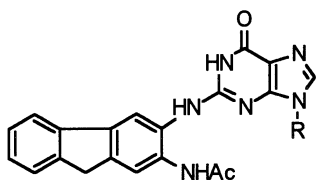
^c The double-stranded form.

significantly to the measured reactivity.⁸ This result shows that d-G residues in double-stranded DNA trap nitrenium ions very inefficiently, on average. The d-G residues within pUC19 do not have identical environments and they may show a range of reactivities toward **2a**, but it is clear from our data that most d-G moieties in pUC19 show very little reactivity toward **2a**.

Table 2 summarizes the reactivities of d-G moieties in various environments with the nitrenium ion **2a** at 0°C. Monomeric d-G is most reactive. It traps **2a** very efficiently ($>50\%$ trapping) at $[d-G]$ as low as 0.1 mM. The reactivity of d-G residues in single-stranded DNA is reduced, but is still substantial. The trapping efficiency at 0.1 mM in d-G residues is about half of that of monomeric d-G. The d-G residues in double-stranded DNA show negligible reactivity toward **2a** with a maximum trapping efficiency at 0.10 mM in d-G residues of about 2.5%.

These results show that the tertiary structure of the DNA double helix significantly inhibits the formation of the C-8 adduct. The magnitude of this inhibition is surprising because the C-8 adduct is apparently formed by rearrangement of an initially formed N-7 adduct, and N-7 of d-G is accessible in the major groove of the DNA double helix.^{8,12} The large bulk of **2a** may play a role in limiting the accessibility of N-7 to this nitrenium ion. This inhibition of the formation of the C-8 adduct may be the reason that treatment of native DNA with **1a** or its precursors leads to the formation of a minor (5–20% compared with the C-8 adduct) N-2 adduct, **7**.^{9a-e,13} This adduct is not detected in studies with d-G or denatured DNA.^{5,9d,14} It appears that this adduct is only detected if the formation of the more abundant C-8 adduct is inhibited. This has important implications with respect to carcinogenesis because the N-2 adduct is more resistant than the more abundant C-8 adduct to excision and repair.^{9,13} Ironically, the resistance of the double helix to formation of the C-8 adduct may make it more susceptible to the formation of the potentially more dangerous N-2 adduct.

Our data show that, *in vivo*, duplex DNA should be fairly resistant to attack by **2a**. Only in cells undergoing DNA replication or transcription is it likely that efficient



7

reaction with **2a** can occur. It is a well known phenomenon that actively growing cells, such as tumor cells and stem cells in their mitotic phase, are more susceptible to anti-cancer drugs that attack DNA.¹⁵ It appears that the same generalization holds true for susceptibility to nitrenium ion-based carcinogens.

EXPERIMENTAL

The synthesis of **1a** has been described previously.¹⁶ Purification of solvents and preparation of buffer solutions have been described.^{3–5} NaN_3 and d-G were obtained commercially and were used without further purification. The DNA hexamer d-ATGCAT was purchased from National Biosciences. In all cases the pH was maintained at 7.5 with low concentration (1–5 mM) $\text{Na}_2\text{HPO}_4\text{--NaH}_2\text{PO}_4$ (9:1) buffer. The ionic strength was maintained at 0.5 with NaClO_4 .

pUC19 was prepared by a general procedure.¹⁷ The DH5 α *E. coli* strain that expresses pUC19 was amplified in a rich medium (5 g l^{-1} yeast extract, 10 g l^{-1} tryptone, 10 g l^{-1} NaCl, pH 7.5, autoclaved for 30 min) containing ampicillin and chloramphenicol. The cells were harvested and lysed with sodium dodecyl sulfate. pUC19 was purified by equilibrium centrifugation in CsCl –ethidium bromide gradients. Concentrations were monitored by UV methods and purity was determined by a densitometric scan of an image of a UV illumination of an ethidium bromide-stained gel. The purity was determined to be 98%.

Product studies. The hydrolysis product **3**, the azide adducts **4** and **5** and the C-8 adduct formed with d-G, **6**, have been characterized previously.^{3,4,14} Authentic samples of all compounds were available. Product yields were determined by HPLC methods with UV detection at 278 or 280 nm.

All product yields were determined by 20 μl injections on to a C-8 Ultrasphere octyl column using a $\text{MeOH--H}_2\text{O}$ eluent (6:4 or 6.5:3.5) buffered with 0.050 M NaOAc--HOAc (1:1) at a flow rate of 1 ml min^{-1} .

Product studies were initiated by a 15 μl injection of a 2.0 mM stock solution of **1a** in DMF into 3.0 ml of the aqueous solution containing NaN_3 , d-G, d-ATGCAT or pUC19 to produce an initial concentration of **1a** of

1.0×10^{-5} M. The concentrations of N_3 , d-G and d-ATGCAT were kept in the range 0.1–1.0 mM. pUC19 was used at a concentration that resulted in a 0.66 mM concentration of d-G residues. All reaction mixtures were incubated at 0, 20 or 30 °C.

A melting curve for d-ATGCAT was obtained by monitoring the UV absorbance at 260 nm for a solution of the oligomer in the temperature range –12 to 70 °C under solvent conditions identical with those used in the product studies. At temperatures below about –5 °C the solution is super-cooled and will freeze spontaneously if disturbed. UV measurements can be made on this solution if care is taken to minimize dust particles in the solution and any shock to the solution.

Kinetics. Kinetic measurements in NaN_3 and d-G solutions have been described.^{3–5} The rate of decomposition of **1a** in 0.9 mM d-ATGCAT at 0 °C was monitored by UV methods at 300 nm. The concentrations and solvent conditions were identical with those used in the product studies.

Acknowledgments

This work was supported by a grant from the American Cancer Society (CN-23K). The authors thank Dr Michael W. Crowder of this Department for his assistance in preparing and purifying pUC19.

REFERENCES

- J. P. Richard and W. P. Jencks. *J. Am. Chem. Soc.* **104**, 4689–4691, 4691–4692 (1982); **106**, 1383–1396 (1984); J. P. Richard, M. E. Rothenburg, W. P. Jencks. *J. Am. Chem. Soc.* **106**, 1361–1372 (1984); D. S. Kemp and M. L. Casey. *J. Am. Chem. Soc.* **95**, 6670–6680 (1973); Z. Rappoport. *Tetrahedron Lett.* 2559–2562 (1979); J. P. Richard, T. L. Amyes and T. Vontor. *J. Am. Chem. Soc.* **113**, 5871–5873 (1991).
- J. C. Fishbein and R. A. McClelland. *J. Am. Chem. Soc.* **109**, 2824–2825 (1987).
- M. Novak, M. J. Kahley, J. Lin, S. A. Kennedy and L. A. Swanegan. *J. Am. Chem. Soc.* **117**, 574–575 (1995); M. Novak, M. J. Kahley, J. Lin, S. A. Kennedy and T. G. James. *J. Org. Chem.* **60**, 8294–8304 (1995).
- M. Novak, M. J. Kahley, E. Eiger, J. S. Helmick and H. E. Peters. *J. Am. Chem. Soc.* **115**, 9453–9460 (1993).
- M. Novak and S. A. Kennedy. *J. Am. Chem. Soc.* **117**, 574–575 (1995).
- P. A. Davidse, M. J. Kahley, R. A. McClelland and M. Novak. *J. Am. Chem. Soc.* **116**, 4513–4514 (1994).
- R. A. McClelland, P. A. Davidse and G. Hadzialic. *J. Am. Chem. Soc.* **117**, 4173–4174 (1995).
- S. A. Kennedy, M. Novak and B. A. Kolb. *J. Am. Chem. Soc.* **119**, 7654–7664 (1997).
- (a) E. Kriek. *Chem. Biol. Interact.* **1** 3–17, (1969); (b) E. Kriek. *Chem Biol Interact.* **3**, 19–28 (1971); (c) J. H. N. Meerman, F. A. Beland and G. J. Mulder. *Carcinogenesis* **2** 413–416, (1981); (d) R. P. P. Fuchs. *Anal. Biochem.* **91**, 663–673, (1978); (e) F. A. Beland, K. L. Dooley and C. D. Jackson. *Cancer Res.* **42**, 1348–1354, (1982); (f) N. Tamora and C. M. King. *Carcinogenesis* **11**, 535–540, (1990); (g) J. H. Nelson, D. Grunberger, C. R. Cantor and I. B. Weinstein. *J. Mol. Biol.* **62**, 331–346, (1971); (h) G. R. Under-

- wood, M. F. Price and R. Shapiro. *Carcinogenesis* **9**, 1817–1821, (1988); (i) M.-S. Lee and C. M. King. *Chem.–Biol. Interact.* **34**, 239–248, (1981); (j) M. L. M. Van de Poll, D. A. M. Van der Hulst, A. D. Bates and J. Meerman. *Carcinogenesis* **11**, 333–339, (1990); (k) R. Shapiro, G. R. Underwood, H. Zawadzka, S. Broyde and B. Hingerty. *Biochemistry* **25**, 2198–2205, (1986).
10. R. A. McClelland, V. M. Kanagasabapathy, N. S. Banait and S. Steenken. *J. Am. Chem. Soc.* **111**, 3966–3972, (1989); **113**, 1009–1014, (1991).
 11. M. Novak, J. N. Zemis. *J. Org. Chem.* **50**, 4661–4663, (1985).
 12. W. G. Humphreys, F. F. Kadlubar and F. P. Guengerich. *Proc. Natl. Acad. Sci. USA* **89**, 8278–8282, (1992).
 13. E. Kriek. *Cancer Res.* **1972** 32, 2042–2048, (1972); J. G. Westra, E. Kriek and H. Hittenhausen. *Chem.–Biol. Interact.* **15**, 149–164, (1976).
 14. E. Kriek, J. A. Miller, U. Juhl and E. C. Miller. *Biochemistry* **6**, 177–182, (1967); F. E. Evans, D. W. Miller and R. A. Levine. *J. Am. Chem. Soc.* **106**, 396–401, (1984).
 15. T. J. Priestman. *Cancer Chemotherapy: An Introduction*, 3rd ed pp 3–26, Springer Berlin, (1989).
 16. F. A. Beland, D. W. Miller and R. K. Mitchum. *J. Chem. Soc., Chem. Commun.* 30–31 (1983); B. A. Smith, J. R. Springfield and H. R. Gutman. *Carcinogenesis* **7**, 405–411, (1986).
 17. J. Sambrook, E. Fitsch and T. Maniatis. *Molecular Cloning A Laboratory Manual*, 2nd ed pp 133–152. Cold Spring Harbor Laboratory Press Plainview NY, (1989).